Torrecillasite, Na(As,Sb)$_4^{3+}$O$_6$Cl, a new mineral from the Torrecillas mine, Iquique Province, Chile: description and crystal structure

A. R. Kampf[1],*, B. P. Nash[2], M. Dini[3] and A. A. Molina Donoso[4]

[1] Mineral Sciences Department, Natural History Museum of Los Angeles County, 900 Exposition Boulevard, Los Angeles, CA 90007, USA
[2] Department of Geology and Geophysics, University of Utah, Salt Lake City, Utah 84112, USA
[3] Pasaje San Agustin 4045, La Serena, Chile
[4] Los Algarrobos 2986, Iquique, Chile

ABSTRACT

The new mineral torrecillasite (IMA2013-112), Na(As,Sb)$_4^{3+}$O$_6$Cl, was found at the Torrecillas mine, Iquique Province, Chile, where it occurs as a secondary alteration phase in association with anhydrite, cinnabar, gypsum, halite, lavendulan, magnesiokoritnigite, marcasite, quartz, pyrite, scorodite, wendwilsonite and other potentially new As-bearing minerals. Torrecillasite occurs as thin colourless prisms up to 0.4 mm long in jack-straw aggregates, as very thin fibres in puff balls and as massive intergrowths of needles. Prisms are elongated on [100] with diamond-shaped cross-section and irregular terminations. Crystals are transparent, with adamantine lustre and white streak. The Mohs hardness is 2½, tenacity is brittle and fracture is irregular. Cleavage on (001) is likely. The calculated density is 4.056 g cm^{-3}. Optically, torrecillasite is biaxial (−) with α = 1.800(5), β = 1.96(1), γ = 2.03(calc.) (measured in white light). The measured 2V is 62.1(5)º, no dispersion or pleochroism were observed, the optical orientation is X = **c**, Y = **b**, Z = **a**. The mineral is very slowly soluble in H$_2$O, slowly soluble in dilute HCl and rapidly soluble in concentrated HCl. The empirical formula, determined from electron-microprobe analyses, is (Na$_{1.03}$Mg$_{0.02}$)$_{\Sigma1.05}$(As$_{3.39}$Sb$_{0.62}$)$_{\Sigma4.01}$O$_{6.07}$Cl$_{0.93}$. Torrecillasite is orthorhombic, *Pmcn*, a = 5.2580(9), b = 8.0620(13), c = 18.654(3) Å, V = 790.7(2) Å^3 and Z = 4. The eight strongest X-ray powder diffraction lines are [d_{obs} Å(*I*)(*hkl*)]: 4.298(33)(111), 4.031(78)(014,020), 3.035(100)(024,122), 2.853(39)(115,123), 2.642(84)(124,200), 2.426(34)(125), 1.8963(32)(225) and 1.8026(29)(0·1·10,233). The structure, refined to R_1 = 4.06% for 814 F_o >4σF reflections, contains a neutral, wavy As$_2$O$_3$ layer parallel to (001) consisting of As^{3+}O$_3$ pyramids that share O atoms to form six-membered rings. Successive layers are flipped relative to one another and successive interlayer regions contain alternately either Na or Cl atoms. Torrecillasite is isostructural with synthetic orthorhombic NaAs$_4$O$_6$Br.

KEYWORDS: torrecillasite, new mineral, arsenite, crystal structure, Torrecillas mine, Chile.

Introduction

THE Torrecillas mine, in the northern Atacama Desert of Chile, is a small, long-inactive As mine

* E-mail: akampf@nhm.org

consisting of several small pits and a shaft on Torrecillas Hill, overlooking the Pacific Ocean. The deposit was probably discovered and first mined during the guano mining boom of the early 19th century. During that period, the Peruvian Government owned and claimed several guano fields along the Chilean coast in the Iquique and

Tarapacá provinces, including the prolific Huanillos, Chanabaya and Pabellón de Pica deposits, which are not far from the Torrecillas area (Mortimer *et al.*, 1971). The guano mines under Peruvian administration, were exploited mainly by English companies. Torrecillas mine was probably abandoned several years prior to 1950 (Pimentel, 1978).

The new mineral torrecillasite, described herein and named for the locality, is the fourth new mineral species described from the mine. The discoveries of all four new species [the others being leverettite (Kampf *et al.*, 2013*b*), magnesio-koritnigite (Kampf *et al.*, 2013*a*) and canutite (Kampf *et al.*, 2014)] and several others, yet to be described, are the result of recent field investigations and collecting at the locality by one of the authors (AAMD). An image of the locality is provided by Kampf *et al*. (2013*a*) and appears on the cover of the December 2013 issue of *Mineralogical Magazine*.

The new mineral and the name have been approved by the International Mineralogical Association (IMA2013-112). The description is based upon four cotype specimens that are deposited in the collections of the Natural History Museum of Los Angeles County, 900 Exposition Boulevard, Los Angeles, CA 90007, USA, catalogue numbers 64079, 64080, 64081 and 64082.

Occurrence

The Torrecillas mine is located on Torrecillas Hill, Iquique Province, Tarapacá Region, Chile (~20°58′13″S 70°8′17″W). Four different rock units are exposed on the hill. Rocks of the Coastal Range Batholith (mainly gabbros) extend from the seashore to the Pan-American Road along the base of the hill. At the foot of the hill is a small area of contact metamorphic rocks in which garnet crystals occur in metamorphosed shales. Higher on the hill, rocks are predominantly andesites and porphyritic lavas of the Jurassic La Negra Formation. The Torrecillas deposit, which the Torrecillas mine exploits, consists of two main veins rich in secondary As and Cu minerals that intersect metamorphosed marine shales and lavas. These veins are related genetically to the above-mentioned andesites and porphyritic lavas of the La Negra Formation. More information on the geology and mineralogy of the area is provided by Gutiérrez (1975).

The rare secondary chlorides, arsenates and arsenites have been found at three main sites on the hill: an upper pit measuring ~8 m long and 3 m deep, a lower pit ~100 m from the upper pit and measuring ~5 m long and 3 m deep and a mine shaft adjacent to the lower pit and lower on the hill. The torrecillasite was first found by one of the authors (AAMD) in early 2012 in boulders on the hill slope just below the mine shaft and he collected additional material there in mid-2013. The boulders appear to represent the oxidation cap of the deposit.

Torrecillasite is associated with anhydrite, cinnabar, gypsum, halite, lavendulan, magnesio-koritnigite (Kampf *et al.*, 2013*a*), marcasite, quartz, pyrite, scorodite and wendwilsonite. Leverettite (Kampf *et al.*, 2013*b*), canutite (Kampf *et al.*, 2014) and several other potentially new arsenate and arsenite minerals, currently under study, have also been found at the locality. The secondary assemblages at the Torrecillas deposit are interpreted as having formed from the

FIG. 1. Backscatter scanning electron microscope image of torrecillasite crystals.

TABLE 1. Electron microprobe analyses of torrecillasite

Constituent	Wt.%	Range	SD
Na$_2$O	6.56	6.07−7.04	0.36
MgO	0.15	0.12−0.18	0.02
As$_2$O$_3$	68.64	65.40−71.85	2.37
Sb$_2$O$_3$	18.43	15.66−20.72	2.14
Cl	6.75	6.37−7.24	0.36
O=Cl	−1.52		
Total	99.01		

oxidation of native As and other As-bearing primary phases, followed by later alteration by saline fluids derived from evaporating meteoric water under hyperarid conditions (e.g. Cameron *et al.*, 2007).

Physical and optical properties

Torrecillasite occurs as thin colourless prisms up to 0.4 mm long in jack-straw aggregates (Fig. 1), as very thin fibres in puff balls and as massive intergrowths of needles. Prisms are elongated on [100] with diamond-shaped cross-section and irregular terminations. Crystals are transparent, with adamantine lustre and white streak. The Mohs hardness is 2½ based on scratch tests. The tenacity is brittle and the fracture is irregular. Cleavage was not observed, but is likely on (001) based on the crystal structure. The density could not be measured because there is insufficient material for direct measurement and crystals are nearly invisible in Clerici solution. The mineral is very slowly soluble in H$_2$O (hours), slowly soluble in dilute HCl (minutes) and rapidly soluble in concentrated HCl (seconds).

The calculated density is 4.056 g cm^{-3} based on the empirical formula. Optically, torrecillasite is biaxial (−) with α = 1.800(5), β = 1.96(1), γ = 2.03(calc.) (measured in white light). The 2V measured from extinction data using *EXCALIBR* (Gunter *et al.*, 2004) is 62.1(5)º. Because liquids with index of refraction >2 were unavailable, γ was calculated from α, β and 2V. No dispersion was observed and torrecillasite is nonpleochroic. The optical orientation is X = **c**, Y = **b**, Z = **a**.

Composition

Quantitative analyses (six points over four crystals) were performed at the University of Utah using a Cameca SX-50 electron microprobe with four wavelength-dispersive spectrometers. Analytical conditions were 15 kV accelerating voltage, 10 nA beam current and a beam diameter of 10 μm. Counting times were 20 s on peak and 10 s on + and − background. No other elements were detected by energy dispersive spectroscopy. Other possible elements were sought by electron microprobe analysis, but none was above the detection limit. Raw X-ray intensities were corrected for matrix effects with a φ(ρz) algorithm (Pouchou and Pichoir, 1991). The standards used were albite for Na, diopside for Mg, synthetic GaAs for As, synthetic GaSb for Sb and tugtupite for Cl. Analytical data are given in Table 1. The ranges for the As and Sb analyses reflect Sb substitution for As, as is also indicated by the crystal structure refinement (see below).

The empirical formula based on O + Cl = 7 is (Na$_{1.03}$Mg$_{0.02}$)$_{\Sigma 1.05}$(As$_{3.39}$Sb$_{0.62}$)$_{\Sigma 4.01}$O$_{6.07}$Cl$_{0.93}$. The simplified structural formula is NaAs$_4^{3+}$O$_6$Cl, which requires Na$_2$O 6.82, As$_2$O$_5$ 87.13, Cl 7.81, O = Cl −1.76, total 100 wt.%. The Gladstone-Dale compatibility index 1 − (K$_P$/K$_C$) is 0.012 for the empirical formula, in the range of superior compatibility (Mandarino, 2007).

X-ray crystallography and structure refinement

Both powder and single-crystal X-ray studies were carried out using a Rigaku R-Axis Rapid II curved imaging plate microdiffractometer, with monochromatic MoKα radiation. For the powder-diffraction study a Gandolfi-like motion on the φ and ω axes was used to randomize the sample and observed *d* spacings and intensities were derived by profile fitting using *JADE 2010* software (Materials Data, Inc.). The powder data presented in Table 2 show good agreement with the pattern calculated from the structure determination. Unit-cell parameters refined from the powder data using *JADE 2010* with whole-pattern fitting are *a* = 5.2677(9), *b* = 8.0412(15), *c* = 18.626(3) Å and *V* = 789.0(2) Å^3.

The Rigaku *CrystalClear* software package was used for processing structure data, including the application of both numerical and empirical absorption corrections, the latter being a multi-scan correction using *ABSCOR* (Higashi, 2001). The structure was solved by direct methods using *SIR2004* (Burla *et al.*, 2005), after which the coordinates were transformed to conform with those reported for synthetic NaAs$_4$O$_6$Br (Pertlik,

TABLE 2. Powder X-ray data for torrecillasite*.

I_{obs}	d_{obs}	d_{calc}	I_{calc}	hkl		I_{obs}	d_{obs}	d_{calc}	I_{calc}	hkl
27	4.654	4.6635	38	0 0 4				1.9700	3	0 4 2
		4.5803	3	1 0 2		7	1.9534	1.9480	10	2 1 6
33	4.298	4.2863	62	1 1 1				1.9173	4	0 4 3
78	4.031	4.0368	100	0 1 4		32	1.8936	1.8964	22	2 2 5
		4.0310	14	0 2 0				1.8725	7	1 4 1
		3.9825	3	1 1 2				1.8448	3	1 4 2
		3.9401	10	0 2 1		29	1.8026	1.8174	11	0·1·10
		3.7002	8	0 2 2				1.7989	14	2 3 3
24	3.597	3.5939	27	1 1 3		2	1.7489	1.7445	3	2 0 8
3	3.398	3.3858	6	0 1 5		11	1.7144	1.7177	5	1·1·10
23	3.168	3.2020	13	1 1 4				1.7055	5	3 1 1
		3.1530	33	1 2 1				1.6975	4	2 2 7
		3.1090	6	0 0 6		14	1.6765	1.6784	4	2 3 5
100	3.035	3.0496	8	0 2 4				1.6700	9	1 3 8
		3.0260	49	1 2 2				1.6100	3	1 4 6
39	2.853	2.8467	15	1 1 5		27	1.6003	1.6075	12	0 4 7
		2.8447	18	1 2 3				1.6014	4	3 2 1
21	2.707	2.7381	19	0 2 5				1.5955	7	2 1 9
		2.6762	57	1 0 6				1.5888	6	0 5 2
84	2.642	2.6380	43	1 2 4				1.5840	6	3 2 2
		2.6290	56	2 0 0				1.5765	3	2 4 2
10	2.544	2.5399	5	1 1 6		22	1.5593	1.5608	6	0 5 3
		2.5304	4	2 0 2				1.5562	4	3 2 3
		2.4668	5	0 3 3		16	1.5266	1.5358	7	2 3 7
34	2.426	2.4285	22	1 2 5				1.5268	9	3 0 6
		2.3929	11	1 3 0				1.5196	7	3 2 4
24	2.377	2.3735	34	1 3 1		27	1.4972	1.4983	15	1·2·11
		2.3318	3	0 0 8				1.4950	16	2·1·10
19	2.315	2.3178	11	1 3 2		25	1.4656	1.4761	4	3 2 5
		2.2902	5	2 0 4				1.4645	5	1 4 8
		2.2800	4	1 1 7				1.4635	11	3 3 1
		2.2332	9	1 3 3				1.3803	3	3 1 8
18	2.213	2.2230	5	0 2 7		14	1.3689	1.3714	12	2 4 7
		2.2030	18	2 1 4				1.3598	9	2 5 2
11	2.0696	2.0765	11	2 1 5		10	1.3422	1.3421	10	2 5 3
		2.0607	11	1 1 8				1.3275	3	3 3 6
11	2.0045	2.0075	8	2 0 6				1.3249	3	1·4·10
		1.9912	3	2 2 4		16	1.3179	1.3145	10	4 0 0

* Only calculated lines with intensities ⩾3 are shown.

1987), with which torrecillasite is isostructural. *SHELXL-2013* (Sheldrick, 2008) was used for the refinement of the structure.

The occupancies of the four independent *As* sites were refined with joint occupancies by As and Sb. The *As*2 and *As*3 sites refined to full occupancy by only As, while the *As*1 site refined to 0.586(10) As and 0.414(10) Sb and the *As*4 site refined to 0.930(9) As and 0.070(9) Sb. As a crosscheck, the occupancies of the *As* sites were also analysed using the program *OccQP* (Wright et al. 2001), which uses quadratic equations in a constrained least-squares formulation to optimize occupancy assignments based upon site scattering, chemical composition, charge balance, bond valence and cation-anion bond lengths. *OccQP* calculations with the number of As and Sb atoms per formula unit set to correspond to the EPMA results provided the following occupancies: *As*1: ($As_{0.564}Sb_{0.436}$), *As*2: ($As_{0.977}Sb_{0.023}$), *As*3: ($As_{0.953}Sb_{0.047}$), *As*4: ($As_{0.887}Sb_{0.113}$). Our final refinement is based upon the aforementioned

TABLE 3. Data collection and structure-refinement details for torrecillasite.

Diffractometer	Rigaku R-Axis Rapid II
X-ray radiation/power	$MoK\alpha$ ($\lambda = 0.71075$ Å)/50 kV, 40 mA
Temperature	298(2) K
Structural Formula	$Na(As_{3.38}Sb_{0.62})_{\Sigma4.00}O_6Cl$
Space group	$Pmcn$
Unit-cell dimensions	$a = 5.2580(9)$ Å
	$b = 8.0620(13)$ Å
	$c = 18.654(3)$ Å
	$V = 790.7(2)$ Å^3
Z	4
Density (for above formula)	4.058 g cm^{-3}
Absorption coefficient	16.631 mm^{-1}
$F(000)$	876.6
Crystal size (μm)	$140 \times 15 \times 5$
θ range	3.34 to 27.46º
Index ranges	$-6 \leqslant h \leqslant 5$, $-10 \leqslant k \leqslant 10$, $-23 \leqslant l \leqslant 22$
Reflections collected/unique	4605/1000; $R_{int} = 0.062$
Reflections with $F_o > 4\sigma(F)$	814
Completeness to θ = 27.46º	99.4%
Refinement method	Full-matrix least-squares on F^2
Parameters refined	69
GoF	1.198
Final R indices [$F_o > 4\sigma(F)$]	$R_1 = 0.0406$, $wR_2 = 0.0667$
R indices (all data)	$R_1 = 0.0561$, $wR_2 = 0.0703$
Largest diff. peak/hole	$+1.141/-1.254$ e A^{-3}

$R_{int} = \Sigma|F_o^2 - F_o^2(\text{mean})|/\Sigma[F_o^2]$. GoF $= S = \{\Sigma[w(F_o^2 - F_c^2)^2]/(n-p)\}^{1/2}$. $R_1 = \Sigma||F_o| - |F_c||/\Sigma|F_o|$.
$wR_2 = \{\Sigma[w(F_o^2 - F_c^2)^2]/\Sigma[w(F_o^2)^2]\}^{1/2}$; $w = 1/[\sigma^2(F_o^2) + (aP)^2 + bP]$
where a is 0, b is 5.406 and P is $[2F_c^2 + \text{Max}(F_o^2, 0)]/3$.

refined site occupancies, rather than those computed using *OccQP*.

Data collection and refinement details are given in Table 3, atom coordinates and displacement parameters in Table 4, selected bond distances in Table 5 and a bond-valence analysis in Table 6.

Description of the structure

The structure of torrecillasite (Fig. 2) contains a neutral, wavy As_2O_3 layer parallel to (001) consisting of $As^{3+}O_3$ pyramids that share O atoms to form six-membered rings. Successive layers are flipped relative to one another and successive interlayer regions contain alternately either Na or Cl atoms. The Na and Cl nestle above and below the centres of half of the six-membered rings in each As_2O_3 layer. Besides the three short As–O3 bonds, which define the $As^{3+}O_3$ pyramids, the As^{3+} cations also form much longer bonds to Cl atoms in the interlayer region and/or to O atoms in the same As_2O_3 layer. This is typical coordination geometry for As^{3+} due to its lone-pair electrons. Na is coordinated to 8 O atoms (6 in the As_2O_3 layer to which it is closest and 2 in the next As_2O_3 layer) and to one Cl atom, with the Na–Cl bond extending through the centre of a six-membered ring in the As_2O_3 layer. The short As–O bonds within the As_2O_3 layer are much stronger than the other bonds in the structure, especially the very long As–O bonds, suggesting the likelihood of a perfect (001) cleavage.

As noted above, torrecillasite is isostructural with the orthorhombic synthetic phase $NaAs_4O_6Br$ (Pertlik, 1987). Other compounds with the general formula MAs_4O_6X (M = K, NH_4; X = Cl, Br, I) were reported by Pertlik (1988) to be hexagonal and to possess planar As_2O_3 sheets with interlayer regions containing M cations alternating with interlayer regions containing halogen atoms. The recently described mineral lucabindiite, $(K,NH_4)As_4O_6(Cl,Br)$, (Garavelli *et al.*, 2013; IMA2011-010) is isostructural with the latter compounds.

TABLE 4. Atom coordinates and displacement parameters (Å²) for torrecillasite.

	x/a	y/b	z/c	U_{eq}	U^{11}	U^{22}	U^{33}	U^{23}	U^{13}	U^{12}
Na	¾	0.4002(5)	0.5588(2)	0.0318(10)	0.033(3)	0.035(2)	0.028(2)	−0.0014(19)	0	0
As1*	¾	0.16859(10)	0.87893(5)	0.0241(3)	0.0188(5)	0.0250(5)	0.0285(5)	−0.0022(4)	0	0
As2	¾	0.65653(12)	0.04509(6)	0.0227(3)	0.0180(5)	0.0216(5)	0.0285(6)	−0.0019(4)	0	0
As3	¾	0.41702(12)	0.18118(5)	0.0197(3)	0.0160(5)	0.0211(5)	0.0220(5)	0.0004(4)	0	0
As4*	¾	0.78414(12)	0.82924(5)	0.0212(3)	0.0157(5)	0.0223(5)	0.0257(6)	−0.0030(4)	0	0
O1	¾	0.9400(8)	0.8994(4)	0.0254(16)	0.029(4)	0.023(3)	0.025(4)	0.002(3)	0	0
O2	¼	0.3831(8)	0.8607(3)	0.0253(16)	0.030(4)	0.020(3)	0.026(4)	0.003(3)	0	0
O3	0.0010(9)	0.6680(5)	0.8745(2)	0.0239(11)	0.018(2)	0.029(3)	0.025(2)	0.001(2)	0.003(2)	0.003(2)
O4	0.9978(10)	0.1930(6)	0.9519(2)	0.0301(12)	0.027(3)	0.036(3)	0.027(3)	0.005(2)	−0.003(2)	−0.011(2)
Cl	¾	0.4904(3)	0.71233(15)	0.0350(7)	0.0286(14)	0.0367(15)	0.0397(15)	−0.0118(12)	0	0

* Refined site occupancies: As1: As/Sb = 0.586/0.414(10); As4: As/Sb = 0.930/0.070(9).

TABLE 5. Selected bond distances (Å) for torrecillasite.

As1–O1	1.882(7)	As2–O2	1.785(6)	As3–O2	1.791(6)
As1–O4 (×2)	1.894(5)	As2–O4 (×2)	1.798(5)	As3–O3 (×2)	1.806(4)
As1–O2 (×2)	3.165(4)	As2–O3 (×2)	3.287(4)	As3–Cl	3.336(3)
As1–Cl (×2)	3.446(2)	<As2–φ>	2.391	As3–Cl (×2)	3.379(2)
<As1–φ>	2.699			<As3–φ>	2.583
Na–O4 (×2)	2.497(6)	Cl–Na	2.956(5)	As4–O1	1.814(7)
Na–O3 (×2)	2.602(6)	Cl–As4 (×2)	3.206(2)	As4–O3 (×2)	1.826(5)
Na–O4 (×2)	2.715(6)	Cl–As4	3.219(3)	As4–Cl (×2)	3.206(2)
Na–O1 (×2)	2.761(2)	Cl–As3	3.336(3)	As4–Cl	3.219(3)
Na–Cl	2.956(5)	Cl–As3 (×2)	3.379(2)	<As4–φ>	2.516
<Na–φ>	2.678	Cl–As1 (×2)	3.446(2)		

TABLE 6. Bond-valence analysis for torrecillasite. Values are expressed in valence units (vu).

	O1	O2	O3	O4	Cl	Σ_c
Na	0.075 ×2↓→		0.115 ×2→	0.153 ×2→	0.113 0.085 ×2→	0.969
As1	0.911	0.041 ×2↓→		0.884 ×2→	0.040 ×2↓→	2.841
As2		1.011	0.017 ×2→	0.976 ×2→		2.997
As3		0.995	0.955 ×2→		0.042 0.037 ×2↓→	3.021
As4	0.959		0.929 ×2→		0.062 ×2↓→ 0.060	3.001
Σ_a	2.020	2.088	2.016	2.098	0.493	

Multiplicities indicated by ×↓→; bond strengths based on assigned site occupancies; Na^+–O and As^{3+}–O bond strengths from Brown and Altermatt (1985); As^{3+}–Cl bond strengths from Brese and O'Keeffe (1991); Sb^{3+}–O bond strengths from Mills *et al.* (2009).
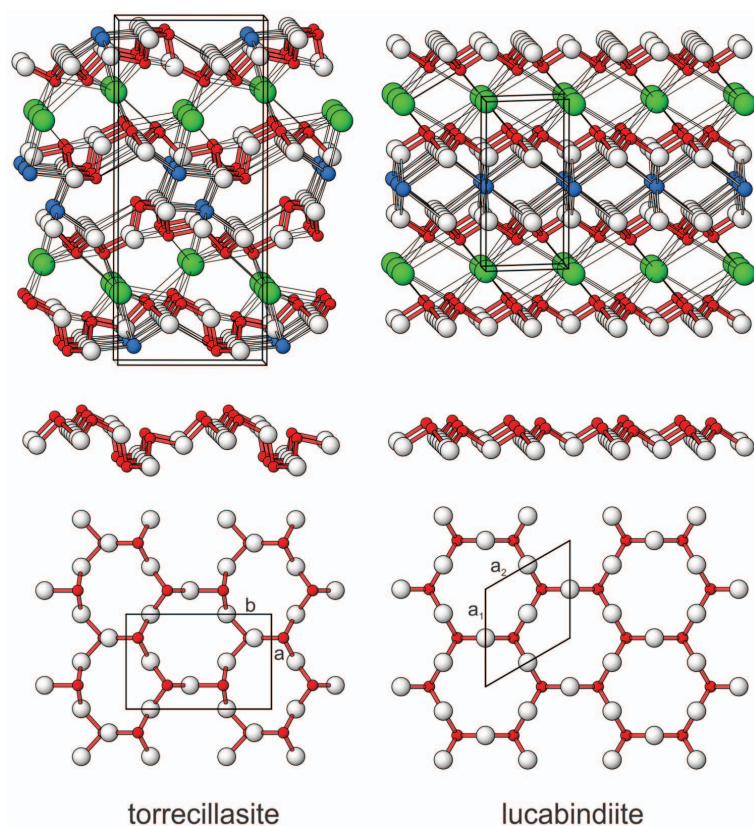

FIG. 2. The structures of torrecillasite and lucabindiite. *Upper*: structures viewed with *c* axis vertical and *a* axis approximately towards the observer; *middle*: As_2O_3 sheets viewed on edge (*c* axis vertical). *Lower*: As_2O_3 sheets viewed along *c* axis. As atoms in red, O atoms in white, large cations (Na, K, NH$_4$) atoms in blue and halide (Cl, Br) atoms in green. Short As–O bonds are shown as red sticks, long As–O bonds as thin black lines and (Na,K,NH$_4$)–O bonds as white sticks. Unit-cell outlines are shown as thick black lines.

The As_2O_3 layers in all of these compounds consist of AsO_3 pyramids that share O atoms to form six-membered rings. Besides the obvious geometric difference between the two types of layers (wavy for the orthorhombic MAs_4O_6X phases and planar for the hexagonal MAs_4O_6X phases), the layers also differ topologically. In the planar layer, all of the As apices point in the same direction, while in the wavy layer, one of the four As apices (As2) points in the opposite direction. The structures and layers of torrecillasite and lucabindiite are compared in Fig. 2.

The bond-valence analysis (Table 6) exhibits one striking anomaly. The bond-valence sum (BVS) for the Cl site is 0.493 vu. Interestingly, it is noteworthy that very low BVS values are found for the Br site in $NaAs_4O_6Br$ (0.657 vu) and the Cl site ($Cl_{0.5}Br_{0.3}F_{0.2}$) in lucabindiite (0.309 vu). The very low BVS values for the X sites in these structures are probably related to the strong repulsive effects of the As^{3+} lone-pair electrons, which are directed into the interlayer space surrounding the X sites.

Finally, a comment about the joint As/Sb occupancies in the As sites of the torrecillasite structure seems warranted. Given the similar stereochemistry of As^{3+} and Sb^{3+} (with a relatively small difference in radius), the articulating nature of the As/Sb layer and the weak layer-to-layer connectivity through a soft Cl sandwich, there appears to be no obvious restraint on the extent of Sb substitution. The Sb-ordering preference indicated, i.e. As1 > As4 > As3 = As2, very probably helps to reduce strain within the As/Sb layer, in conjunction with the connectivity to the flanking Na atoms. An all-Sb^{3+} analogue, $NaSb_4O_6Cl$, appears possible and would clearly warrant separate species status. With increasing Sb content, toward the mid-point in a hypothetical $NaAs_4O_6Cl-NaSb_4O_6Cl$ series, an intermediate phase with Sb dominating the $As1$ site is likely to exist and one with Sb dominating both the $As1$ and $As4$ sites may exist; however, we do not recommend that such intermediate phases be granted separate species status; i.e. we recommend that separate species status only be afforded to a phase in which total Sb is greater than total As.

Acknowledgements

References

Brese, N.E. and O'Keeffe, M. (1991) Bond-valence parameters for solids. *Acta Crystallographica*, **B47**, 192−197.

Brown, I.D. and Altermatt, D. (1985) Bond-valence parameters from a systematic analysis of the inorganic crystal structure database. *Acta Crystallographica*, **B41**, 244−247.

Burla, M.C., Caliandro, R., Camalli, M., Carrozzini, B., Cascarano, G.L., De Caro, L., Giacovazzo, C., Polidori, G. and Spagna, R. (2005) *SIR2004*: an improved tool for crystal structure determination and refinement. *Journal of Applied Crystallography*, **38**, 381−388.

Cameron, E.M., Leybourne, M.I. and Palacios, C. (2007) Atacamite in the oxide zone of copper deposits in northern Chile: involvement of deep formation waters? *Mineralium Deposita*, **42**, 205−218.

Garavelli, A., Mitolo, D., Pinto, D. and Vurro, F. (2013) Lucabindiite, $(K,NH_4)As_4O_6(Cl,Br)$, a new fumarole mineral from the "La Fossa" crater at Vulcano, Aeolian Islands, Italy. *American Mineralogist*, **98**, 470−477.

Gunter, M.E., Bandli, B.R., Bloss, F.D., Evans, S.H., Su, S.C. and Weaver, R. (2004) Results from a McCrone spindle stage short course, a new version of *EXCALIBR*, and how to build a spindle stage. *The Microscope*, **52**, 23−39.

Gutiérrez, H. (1975) *Informe sobre una rápida visita a la mina de arsénico nativo, Torrecillas*. Instituto de Investigaciones Geológicas, Iquique, Chile.

Higashi, T. (2001) *ABSCOR*. Rigaku Corporation, Tokyo.

Kampf, A.R., Nash, B.P., Dini, M. and Molina Donoso, A.A. (2013a) Magnesiokoritnigite, $Mg(AsO_3OH)·H_2O$, from the Torrecillas mine, Iquique Province, Chile: the Mg-analogue of koritnigite. *Mineralogical Magazine*, **77**, 3081−3092.

Kampf, A.R., Sciberras, M.J., Williams, P.A., Dini, M. and Molina Donoso, A.A. (2013b) Leverettite from the Torrecillas mine, Iquique Provence, Chile: the Co-analogue of herbertsmithite *Mineralogical Magazine*, **77**, 3047−3054.

Kampf, A.R., Mills, S.J., Hatert, F., Nash, B.P., Dini, M. and Molina Donoso, A.A. (2014) Canutite, $NaMn_3[AsO_4]_2[AsO_2(OH)_2]$, a new protonated alluaudite-group mineral from the Torrecillas mine, Iquique Province, Chile. *Mineralogical Magazine*, **78**, (in press).

Mandarino, J.A. (2007) The Gladstone-Dale compatibility of minerals and its use in selecting mineral

species for further study. *The Canadian Mineralogist*, **45**, 1307−1324.

Mills, S.J., Christy, A.G., Chen, E.C.-C. and Raudsepp, M. (2009) Revised values of the bond valence parameters for [6]Sb(V)−O and [3−11]Sb(III)−O. *Zeitschrift für Kristallographie*, **224**, 423−431.

Mortimer, C., Saric, N. and Cáceres, R. (1971) *Apuntes sobre algunas minas de la región costera de la provincia de Tarapacá*. Instituto de Investigaciones Geológicas, Santiago de Chile, Chile.

Pimentel, F. (1978) *Proyecto Arsenico Torrecillas*. Instituto de Investigaciones Geológicas, Iquique, Chile.

Pertlik, F. (1987) The crystal structure of NaAs$_4$O$_6$Br. *Journal of Solid State Chemistry*, **70**, 225−228.

Pertlik, F. (1988) The compounds KAs$_4$O$_6$X (X = Cl, Br, I) and NH$_4$As$_4$O$_6$X (X = Br, I): hydrothermal syntheses and structure determinations. *Monatshefte für Chemie*, **119**, 451−456.

Pouchou, J.-L. and Pichoir, F. (1991) Quantitative analysis of homogeneous or stratified microvolumes applying the model "*PAP*". Pp. 3l−75 in: *Electron Probe Quantitation* (K.F.J. Heinrich and D.E. Newbury, editors). Plenum Press, New York.

Sheldrick, G.M. (2008) A short history of *SHELX*. *Acta Crystallographica*, **A64**, 112−122.

Wright, S.E., Foley, J.A. and Hughes, J.M. (2001) Optimization of site occupancies in minerals using quadratic programming. *American Mineralogist*, **85**, 524−531.